HHS Public Access

Author manuscript

J Struct Biol. Author manuscript; available in PMC 2019 April 01.

Published in final edited form as:

J Struct Biol. 2018 April ; 202(1): 13–24. doi:10.1016/j.jsb.2017.11.014.

Direct Regulation of p190RhoGEF by Activated Rho and Rac GTPases

Olugbenga Dada[a], **Stephen Gutowski**[a], **Chad A. Brautigam**[b,c], **Zhe Chen**[b], and **Paul C. Sternweis**[a,*]

[a]Department of Pharmacology, The University of Texas Southwestern Medical Center, 6001 Forest Park Road, Dallas, Texas 75390, USA

[b]Department of Biophysics, The University of Texas Southwestern Medical Center, 6001 Forest Park Road, Dallas, Texas 75390, USA

[c]Department of Microbiology, The University of Texas Southwestern Medical Center, 6001 Forest Park Road, Dallas, Texas 75390, USA

Abstract

Rho family GTPases regulate a wide range of cellular processes. This includes cellular dynamics where three subfamilies, Rho, Rac, and Cdc42, are known to regulate cell shape and migration though coordinate action. Activation of Rho proteins largely depends on Rho Guanine nucleotide Exchange Factors (RhoGEFs) through a catalytic Dbl homology (DH) domain linked to a pleckstrin homology (PH) domain that subserves various functions. The PH domains from Lbc RhoGEFs, which specifically activate RhoA, have been shown to bind to activated RhoA. Here, p190RhoGEF, is shown to also bind Rac1•GTP. Crystal structures reveal that activated Rac1 and RhoA use their effector-binding surfaces to associate with the same hydrophobic surface on the PH domain. Both activated RhoA and Rac1 can stimulate exchange of nucleotide on RhoA by localization of p190RhoGEF to its substrate, RhoA•GDP, *in vitro*. The binding of activated RhoA provides a mechanism for positive feedback regulation as previously proposed for the family of Lbc RhoGEFs. In contrast, the novel interaction between activated Rac1 and p190RhoGEF reveals a potential mechanism for cross-talk regulation where Rac can directly effect stimulation of RhoA. The greater capacity of Rac1 to stimulate p190RhoGEF among the Lbc RhoGEFs suggests functional specialization.

Keywords

RhoGEF; PH domain; GTPase; Crosstalk; Crystal structure; Membrane localization

*Corresponding Author: paul.sternweis@utsouthwestern.edu.

Conflict of interest

The authors declare no conflicts of interest.

1. Introduction

Rho-family GTPases compose a major subfamily of the Ras superfamily of small monomeric GTPases, which play key roles in controlling various aspects of cell behavior through integral signal transduction pathways. RhoA, Rac1, and Cdc42 are the most well characterized Rho GTPases due to their prominent roles in the regulation of the actin cytoskeleton, cell migration, and cell division. As with most monomeric GTPases, Rho proteins act as molecular switches by adopting different conformational states when bound to either GDP or GTP.

Regulation of the Rho GTPases is achieved by Rho guanine nucleotide exchange factors (RhoGEFs) and GTPase-activating proteins (RhoGAPs). Numerous RhoGEFs catalyze the exchange of GDP for GTP on the Rho GTPases, which activates the proteins for subsequent regulation of downstream effectors. RhoGAPs enhance hydrolysis of the bound GTP on Rho, thus inactivating the GTPases. The dynamic balance between these two regulatory paradigms determines the effective action of specific Rho GTPases and their functional input into coordination of many cellular functions. Detailed properties and mechanisms of these proteins have been extensively reviewed elsewhere (Bos et al., 2007; Cherfils and Zeghouf, 2013; Etienne-Manneville and Hall, 2002; Rossman et al., 2005; Schaefer et al., 2014).

p190RhoGEF, also known as RGNEF (mouse) and designated as ARHGEF28, is an ubiquitously expressed regulator of RhoA (Gebbink et al., 1997). This protein contains the classic tandem DHPH domain motif common to the Dbl (diffuse B-cell lymphoma) family of RhoGEFs, as well as a leucine-rich domain, a zinc-finger region, and a coiled-coil motif (van Horck et al., 2001). The DH (Dbl homology) domains of RhoGEFs catalyze nucleotide exchange on the GTPases, while the PH (pleckstrin homology) domains may facilitate this activity or help localization of the RhoGEFs to their appropriate intracellular locations. p190RhoGEF specifically activates Rho isoforms (RhoA, RhoB, and RhoC), but not Rac1 or Cdc42 (Jaiswal et al., 2011; van Horck et al., 2001). Numerous binding partners for this RhoGEF have been identified including: a direct association of the C-terminal region of focal adhesion kinase (Zhai et al., 2003) and 14-3-3 proteins (Zhai et al., 2001) with sites in the coiled-coil region of p190RhoGEF, and an interaction of the scaffold protein, JIP-1, with a site C-terminal to the coiled-coil region (Meyer et al., 1999). The C-terminal region of p190RhoGEF can also associate with microtubules (van Horck et al., 2001) and the proximal untranslated region of mRNA for the neurofilament light subunit (Cañete-Soler et al., 2001). These binding interactions have suggested the importance of p190RhoGEF in focal adhesion formation, cancer cell motility, and neurodegeneration (Lim et al., 2008; Lin et al., 2005; Yu et al., 2011).

The well-defined domains of RhoGEFs play important roles in the regulation of these proteins. A novel role for the PH domain of RhoGEFs in the Lbc family was first indicated by the novel observation of the interaction between the PH domain of PDZRhoGEF (PRG) and its activated substrate, RhoA•GTPγS (Chen et al., 2010b); the inability of this binding interaction to affect basal stimulation of RhoA, *in vitro*, suggested an alternative mechanism for regulation. This was subsequently demonstrated when activated RhoA was shown to stimulate the activity of PRG by localizing the RhoGEF to the surface of membrane vesicles

containing membrane bound substrate (Medina et al., 2013). Mutating the essential residues on the PH domain necessary for binding activated RhoA attenuated this stimulation. Mutation of this binding site also attenuated the ability of PRG to activate RhoA by overexpression in cells. These observations, both *in vitro* and *in vivo*, were expanded to the other 6 members of the Lbc family of RhoGEFs, including p190RhoGEF, thus defining a general mechanism of positive feedback regulation for these RhoGEFs (Medina et al., 2013). Whether other members of the Rho subfamily of Ras GTPases can bind and regulate Lbc RhoGEFs is unknown.

Herein, we show that the PH domain of p190RhoGEF is also capable of interacting with active forms of Rac1. Crystal structures of the PH domain of p190RhoGEF complexed with either activated RhoA or Rac1 reveal a conserved core binding interface shared between the PH domain and both GTPases. Mutation of residues in the mostly hydrophobic binding interface abolished any observed stimulation of RhoGEF activity by either activated RhoA or Rac1 in phospholipid vesicle assays. The novel stimulation of p190RhoGEF by activated Rac1 suggests a potential signaling mechanism that may initiate a transition in cellular regulation from activation of Rac1 to activation of RhoA.

2. Materials and Methods

2.1. Constructs for expression of proteins

Coding regions of the PH domains of human p190RhoGEF (residues 1049–1194, wildtype or mutant) and PRG (residues 927–1085) along with a C-terminal-His_6 tag were inserted into pGEX-KG-TEV, a pGEX-KG vector containing the protease recognition site for the Tobacco Etch Virus (TEV) between the encoded glutathione S-transferase (GST) and added fusion protein, as described previously (Medina et al., 2013). The expression constructs for full length human RhoA, B, and C and Rac1, 2 and 3, as well as the C-terminally truncated GTPases (RhoA-ΔC, residues 1–181 or Rac1-ΔC, residues 1–182) were generated by subcloning the coding region into the pGEX-KG-TEV vector. Constructs of full length human RhoA and Rac1 with a C-terminal His_6 tag were cloned into the pGEX-KG-TEV vector as described previously (Medina et al., 2013). A construct of full length human RhoA with YFP (yellow fluorescent protein) fused to the N-terminus (YFP-RhoA) was cloned into the pGEX-KG-TEV vector as described previously (Medina et al., 2013). To generate a linked p190-PH-Rac1 construct, the coding region of the p190 PH domain was fused N-terminally to the Rac1-ΔC coding region via a linker consisting of 32 amino acids (GLSGQSSLSSPSALNSLSSPSALNSTASNSTG). A fluorescent PRG-PH domain (CFP-PRG-PH) was generated by inserting the Cerulean fluorescent protein (CFP) in between G1014 and S1015 of the PRG PH coding region. Fluorescent p190-PH (CFP-PH) was created by fusing CFP to the N-terminus of the p190 PH domain with a Gly-Ser linker. Both were cloned into the pGEX-KG-TEV vector. Coding regions of the tandem DHPH domains of human p190 (residues 822–1194), PRG (residues 712–1085), LARG (residues 761–1135), AKAP-Lbc (residues 1919–2333), and mouse p114 (residues 72–444) RhoGEFs were inserted into the pGEX-KG-TEV vector as described previously (Medina et al., 2013).

2.2. Expression and purification of proteins

Proteins were expressed in *E. coli* strain BL21(DE3) cells grown in LB medium and induced at 22 °C overnight with 100 μM isopropyl-β-D-thiogalactopyranoside (IPTG); cells were collected by centrifugation and frozen for future use. Frozen cells from 1 L of medium were thawed and suspended with 50 mL of lysis buffer (50 mM NaHEPES, pH 8.0, 200 mM NaCl, 5 mM β-mercaptoethanol, 10 μM GDP and protease inhibitors (23 μg/ml phenylmethylsulfonyl fluoride, 22 μg/ml N^{α}-*p*-tosyl-*L*-lysine chloromethyl ketone, 22 μg/ml tosylphenylalanyl chloromethyl ketone, 22 μg/ml pepstatin A, 1 μg/ml N^{α}-*p*-tosyl-*L*-arginine methyl ester). Lysozyme (2 mg/ml), DNase I (50 μg/ml) and $MgCl_2$ (5 mM) were added and cells were lysed for 60 min at 4 °C followed by centrifugation at 35,000 rpm to remove particulate material. GST-tagged fusion proteins were extracted from the soluble fraction by affinity chromatography with Glutathione Sepharose 4B (GE Healthcare). Resins with GST-fusion proteins bound were suspended with lysis buffer, then incubated overnight at 4 °C in the presence of TEV protease to remove the GST-tag. His_6-tagged proteins released from the resin by TEV protease were further purified by affinity chromatography with Ni-NTA agarose resin (Qiagen). Enriched proteins were further purified with a Mono Q anion exchange column (GE Healthcare) that had been pre-equilibrated with Buffer A (25 mM NaHEPES, pH 8.0, 5 mM β-mercaptoethanol, and 2 mM $MgCl_2$). Elution was accomplished with a linear gradient of 0 to 0.5 M NaCl in Buffer A. Fractions containing GTPase were supplemented with GDP (10 μM). CFP-PH domains were expressed and purified similarly as described above with the following modifications: expressions were carried out at 24°C overnight; the lysis buffer contains 20 mM NaHEPES, pH 8.0, 50 mM NaCl, 5 mM β-mercaptoethanol and protease inhibitors; a buffer containing 20 mM TrisCl, pH 8.0 and 5 mM β-mercaptoethanol was used in anion exchange chromatography.

2.3. Activation of GTPases with GTPγS

Exchange of GTPγS for bound GDP on purified RhoA or Rac1 was carried out as described (Chen et al., 2008). Briefly, RhoA, Rac1 or the linked p190-PH-Rac1 were exchanged into binding buffer (25 mM NaHEPES, pH 8.0, 1 mM EDTA, 1 mM DTT, 50 mM NaCl, and 10 μM GDP) and concentrated to 200–500 μM. The concentrated proteins were adjusted to 0.5 mM $MgSO_4$ and 1 mM GTPγS, and incubated at room temperature for 24 hours.

2.4. Pulldown assays

Immobilized GST-tagged Rho and Rac proteins were used to compare their relative ability to bind purified His_6-tagged PH domains. The GST-GTPases, either basal (GDP) or preactivated with GTPγS, were mixed with 10 μl of glutathione-Sepharose 4B resin (GE Healthcare) in 100 μl of Buffer A (50 mM NaHEPES, pH 7.5, 50 mM NaCl, 1 mM DTT, 1 mM EDTA, 5 mM $MgCl_2$, 0.3% (v/v) Triton X-100, and 0.01% (w/v) bovine serum albumin) and incubated for 30 min at 4 °C. The resin was washed with Buffer A, and His_6-p190 PH domain was added to the immobilized GST-Rho or Rac in Buffer A (100 μl) containing either 10 μM GDP or 10 μM GTPγS for basal or preactivated Rho or Rac, respectively. The mixtures were incubated for an addition 30 min at 4 °C and the resin rapidly separated by spinning in a microcentrifuge. Supernatants containing free PH domains were removed and the resins rapidly washed four times with 600 μl of cold Buffer

A. PH domains bound to the resins were released by incubating in 30 μl of 15 mM reduced glutathione buffer (75 mM TrisCl, pH 8.6) for 5 min, subjected to SDS-PAGE, and visualized by silver staining or immunoblot analysis using an anti-His_6 monoclonal antibody (R&D Systems).

2.5. ITC Assay

Isothermal titration calorimetry (ITC) was performed utilizing a MicroCal iTC200 (Malvern Instruments). Briefly, all protein samples were exchanged into ITC buffer (25 mM TrisCl, pH 8, 100 mM NaCl, 1 mM $MgCl_2$) by size-exclusion chromatography prior to calorimetric characterization. Contents of the sample cell were stirred continuously at 750 rpm during the experiment. A typical titration of a PH domain with activated RhoA involved 19 injections at 2-min intervals of 2 μl PH (200 or 500 μM) into a sample cell containing 0.2 ml of activated RhoA (20 or 50 μM) at 20 °C. The data were then analyzed by integrating the change in heat caused by injections normalized to the amount of injected proteins, then performing curve fitting based on a 1:1 binding model (A+B <−> AB Heteroassocation) using NITPIC and SEDPHAT software, respectively (Keller et al., 2012; Zhao et al., 2015). All ITC figures were rendered using GUSSI (Brautigam, 2015).

2.6. Analytical ultracentrifugation

Analytical ultracentrifugation (AUC) was utilized to study the interaction of activated RhoA (RhoA•GTPγS) and the PH domain of p190 in a titration series, with [RhoA•GTPγS] held constant at 4 μM, and [p190 PH] varied between 0.4 and 40 μM. For this experiment, five titration points were examined, and protein samples were exchanged into AUC buffer (25 mM NaHEPES, pH 8, 200 mM NaCl, 5 mM $MgCl_2$) by size-exclusion chromatography. To conduct this study, 400 μL of buffer and 400 μl of the RhoA•GTPγS/p190-PH mixtures (which had been equilibrated overnight at 4 °C) were pipetted into the reference and sample sectors, respectively, of a 1.2-cm Epon charcoal-filled dual-sectored centerpiece that had been sandwiched between two sapphire windows. The centrifugation cells were placed in an An50-Ti rotor, which was incubated at 20 °C under vacuum for several hours before centrifugation was started. A Beckman Optima XL-I (Beckman-Coulter, Fullerton, CA) centrifuge was used to perform the experiment using a rotor speed of 50,000 rpm, and the data were collected using the on-board spectrophotometer tuned to a wavelength of 280 nm. The $c(s)$ analyses were carried out using SEDFIT (Schuck, 2000). These analyses were compiled and assembled into a weighted-average sedimentation coefficient isotherm (Dam and Schuck, 2005; Schuck, 2003) using GUSSI (Brautigam, 2015). SEDPHAT (Dam and Schuck, 2005) was used to analyze the isotherm; during this analysis, the sedimentation coefficient of the RhoA•GTPγS:p190-PH complex was fixed at the estimated value of 2.9 S. This latter value agrees roughly with the calculated sedimentation coefficient (García De La Torre et al., 2000) of the complex (2.8 S). All $c(s)$ distribution and isotherm figures were rendered using GUSSI (Brautigam, 2015).

2.7. Formation of the p190-PH•RhoA•GTPγS complexes

The p190-PH:RhoA•GTPγS complexes were purified by size-exclusion chromatography using Superdex 200/75 tandem gel filtration columns (GE Healthcare). Equal moles of RhoA(ΔC)•GTPγS and the PH domain were mixed and then filtered through the gel

filtration columns pre-equilibrated with Buffer B (25 mM TrisCl, pH 8.5, 1 mM DTT, 100 mM NaCl and 1 mM EDTA) and 2 mM $MgCl_2$. Fractions that contained the PH:RhoA•GTPγS complex (molecular weight of approximately 40 kDa as judged by elution volume) were pooled and concentrated using Amicon-Ultra 4 (10 kDa) concentrators (Millipore) to a final concentration of 15 mg/ml. Aliquots (20 μl) of the concentrated complex were flash frozen with liquid nitrogen and stored at −80 °C.

2.8. Crystallization and data collection

All proteins were crystallized by hanging drop vapor diffusion at 20 °C. The p190-PH•RhoA(ΔC)•GTPγS complex was crystallized from 20–24 % (w/v) polyethylene glycol 3350, 100 mM TrisCl, pH 7.5–8.5, and 200 mM NaCl. The fusion protein of p190-PH-Rac1(ΔC)•GTPγS was crystallized from 22 % (w/v) polyethylene glycol 3350 and 100 mM NaHEPES, pH 7.5. Crystals were then cryoprotected with an additional 15 % (v/v) ethylene glycol. Native data were measured at 100 K at the Structural Biology Center (Beamline 19ID) at Argonne National Laboratory. Diffraction data were reduced and scaled using the HKL software package (Otwinowski and Minor, 1997).

2.9. Structure determination and model refinement

Initial phases were generated by molecular replacement using the coordinates of p190-PH (unrefined structure) and RhoA (PDB entry 1A2B) or Rac1 (PDB entry 1MH1) as separate search models, using program PHASER (McCoy et al., 2007). Model building was performed using the program Coot (Emsley et al., 2010). The model was refined using the Phenix software package (Adams et al., 2010). Coordinates and individual Atomic Displacement Parameters (B-factors) were refined. TLS refinement was carried out with the PH:RhoA dataset. Maximum Likelihood was used as the target function during refinement. Putative water molecules within hydrogen bonding distance of at least one protein atom or other water oxygen atoms and with refined B-factors <100 $Å^2$ were included in the model. MolProbity (Chen et al., 2010a) indicates that over 95 % of the residues fall in the most favorable regions of ϕ, ψ conformational space (Ramachandran and Sassiekharan, 1968). Coordinates have been deposited in the Protein Data Bank (Berman et al., 2000) with accession code 6BC0 (p190-PH:RhoA) and 6BC1 (p190-PH:Rac1). Atomic representations were created using Pymol (DeLano, 2002).

2.10. Assays of RhoGEF activity with phospholipid vesicles

Unilamellar phospholipid vesicles doped with nickel chelating lipid were made by extrusion and loaded with His_6-tagged proteins as described previously (Medina et al., 2013). The substrate, His_6-RhoA, was loaded with *N*-methylanthraniloyl-GDP (mant-GDP; Invitrogen) and dissociation of mant-GDP measured by its loss of fluorescence when free in solution as described previously (Medina et al., 2013). Briefly, His_6-RhoA•mant-GDP (1 μM) and His_6-RhoA or His_6-Rac1 proteins as indicated were mixed with vesicles (0.5 mM lipid, ~ 5 nM vesicles) in assay buffer (20 mM NaHEPES, pH 7.5, 200 mM NaCl, 2 mM $MgCl_2$, 5 mM β-mercaptoethanol, and 0.01% (w/v) bovine serum albumin). An alternative paradigm used His_6-RhoA• GDP (1 μM) and binding of mant-GDP where exchange of nucleotide was measured by the increase in fluorescence of bound mant-GDP. All reactions were started

with the addition of RhoGEF proteins and the change in fluorescence was monitored with a Fluorolog-3 spectrofluorometer at 25 °C at λ_{ex} = 356 nm, λ_{em} = 445 nm, and slits = 1/1 nm.

2.11. Competition assay using changes in intermolecular FRET

Intermolecular FRET was measured by association of 1 μM YFP-RhoA•GTPγS with 1 μM CFP-PRG-PH or 2 μM YFP-RhoA•GTPγS and 2 μM CFP-p190-PH. Competition was measured by titration of non-fluorescent activated GTPases or non-fluorescent PH domains. Assays were done in 20 mM NaHEPES, pH 7.5, 1 mM EDTA, 1 mM DTT, 100 mM NaCl, 5 mM $MgCl_2$ in a volume of 140 μl utilizing a Fluorolog-3 fluorometer at 25 degrees at λ_{ex} = 433 nm, λ_{em} scanned from 450 to 560 nm, slits = 1/1 nm. Changes in FRET were reported as the ratio of fluorescence at 525 nm over 475 nm.

3. Results

3.1. Binding of activated RhoA and Rac1 to the PH domain of p190RhoGEF

Recently, we demonstrated that active RhoA binds to a conserved hydrophobic region on the surface of PH domains contained in members of the Lbc family of RhoGEFs (Chen et al., 2010b; Medina et al., 2013). An unexpected observation that was made while exploring these interactions with a simple dot blot assay is that the PH domain from p190RhoGEF could also associate with the activated state of Rac1 (bound to GTP). This is shown by a pulldown experiment with purified proteins in Figure 1A. Comparative binding of the p190 PH domain (p190-PH) to activated RhoA was anticipated from earlier studies (Medina et al., 2013). The smaller amount of PH domain associated with activated Rac1 suggests that the interaction of this GTPase with p190-PH has a lower affinity than with activated RhoA. In both cases, negligible binding of p190-PH to the basal GTPases with bound GDP indicates that this binding is specific for the activated forms.

The binding affinity between the PH domain of p190RhoGEF and RhoA•GTPγS was determined by isothermal titration calorimetry (ITC) where p190-PH was titrated into a sample cell containing activated RhoA (Figure 1B). Analysis of the data indicates that the binding affinity for this interaction is about 2 μM (1.7 μM – 2.6 μM, 68.3% confidence intervals). This value of affinity was supported by analytical ultracentrifugation (AUC) (Figure S1). Determinations of binding affinities between the PH domains of other Lbc family RhoGEFs and RhoA•GTPγS were also measured by ITC and varied about 10 fold (PRG-PH, 1.2 μM; AKAP-Lbc-PH, 3.1 μM; p114-PH, 13 μM), while measurements by competitive binding showed domains with lower affinity extend this range to about 100 fold (see Figure 1 in Chen et al., Data in Brief, submitted).

Attempts to directly measure the binding affinity between p190-PH and Rac1•GTPγS were not successful due to large errors in measuring low heat released by the binding events. Therefore, we utilized a competition approach where untagged GTPases competed with binding of fluorescent YFP-RhoA to CFP-p190-PH. The reduction in FRET by increasing concentrations of untagged GTPase could then produce relative IC50s. As shown in Figure 1C, the relative affinity of Rac1 for p190-PH was 10-fold less than the untagged RhoA suggesting an actual affinity for Rac1•GTPγS binding to p190-PH of about 20 μM. The

ability of p190-PH to bind to both RhoA and Rac1 raised the question of whether the PH domain would bind similarly to the other isoforms of Rho and Rac or show differential selectivity for the isoforms of these GTPases. More extensive pulldown assays showed that p190-PH was also capable of binding to all the tested isoforms of activated Rac (Rac1, Rac2, and Rac3) and Rho (RhoA, RhoB, and RhoC) (Figure S2).

3.2. Overall structures of the p190-PH:RhoA•GTPγS and the p190-PH:Rac1•GTPγS complexes

The p190-PH:RhoA•GTPγS complex was formed by mixing equal molar amounts of nonprenylated, C-terminally truncated RhoA bound to GTPγS and p190-PH in the presence of Mg^{2+}, incubation, and isolation of the stoichiometric complex by size-exclusion chromatography. Crystals were grown by vapor diffusion. The structure of RhoA•GTPγS bound to the PH domain of p190 was determined at a resolution of 2.2 Å by molecular replacement using separate search models for p190-PH (based on an unrefined structure from crystals of the PH domain alone, which was not further pursued), and RhoA (PDB access code 1A2B) (Figure 2). The model was refined to conventional and free crystallographic *R* values of 22.3 % and 28.1 %, respectively. The final atomic model comprises residues 1055–1086, 1090–1114 and 1116–1190 of the p190 PH domain and residues 3–181 of RhoA bound to GTPγS and Mg^{2+}. The remaining residues are disordered. Data collection and refinement statistics are summarized in Table 1.

The relatively low binding affinity between the PH domain of p190 and activated Rac1 bound to GTPγS did not allow isolation of the stoichiometric complex by size-exclusion chromatography. Attempts to directly crystallize a complex from equimolar concentrations of the two proteins were unproductive. Therefore, the C-terminus of p190-PH was fused to the N-terminus of a C-terminally truncated Rac1 via a 32 amino acid linker, and expressed in bacteria as a fusion protein. Crystals were grown by vapor diffusion. While the linker was cleaved during the crystallization process, presumably due to the presence of proteases that co-purified with the fusion protein, a crystal containing both p190-PH and Rac1 was obtained as verified by western blot using anti-p190 and anti-Rac1 antibodies (data not shown). Although the crystal diffracted to 2.54 Å, the data are strongly anisotropic (Table 1). Molecular replacement using separate search models for p190-PH and Rac1 (PDB access code 1MH1) found two p190-PH:Rac1•GTPγS complexes per asymmetric unit (Figure S3). The resolution cutoff for the refinement (2.9 Å) was selected based on visual inspection of electron density maps that was combined with refinements run with variable resolution cutoffs. The model was refined to conventional and free crystallographic R values of 27.2 % and 31.7 %, respectively. One copy of the complex comprised of Chain B (Rac1) and Chain D (PH), hereafter referred to as Complex-BD, is lacking lattice contacts due to the smaller number of intermolecular crystal contacts when compared to the other complex in the asymmetric unit (Figure S3). The calculated buried surface areas in the crystalline lattice showed that 33% of the surface area from Chain A and 30% from Chain C are involved in contacts with adjacent molecules in the lattice, whereas only 20% of the surface area from Chain D and 10% from Chain B are involved in such interactions. This is reflected by the increased real-space R-values, the elevated B-factors for Complex-BD, and the poor electron density maps of Complex-BD. The average atomic displacement parameters described by B-

factors are 34 Å^2 (with a range between 19 and 87 Å^2) and 40 Å^2 (with a range between 14 and 71 Å^2) for Chain A and Chain C, respectively. These values rise to 79 Å^2 (with a range between 50 and 155 Å^2) and 66 Å^2 (with a range between 25 and 127 Å^2) for Chain B and Chain D, respectively. Therefore, Complex-BD, especially Chain B, should not be interpreted in terms of atomic positions and the exact positions of side chains are highly uncertain locally. In spite of this, the electron density map for the complex comprised of Chain A and Chain C (Complex-AC) is excellent, with clear and unambiguous densities for the side chains and bound GTPγS (Figure S4, S5). All figures representing the p190-PH:Rac1 complex are generated with Chain A and Chain C from the refined model. The final atomic model comprises residues 1053–1085 and 1088–1195 of the p190 PH domain and residues 2–177 of Rac1 bound to GTPγS and Mg^{2+}.

Activated RhoA interacts with the C-terminal layer of β-strands in the PH domain of p190RhoGEF (Figure 2). Similar interactions have been observed with the PH domains from other Lbc RhoGEFs when bound to activated RhoA based on structure (see Figures 2 and 3 in Chen et al., Data in Brief, submitted; Chen et al., 2010b) or point mutations (Medina et al., 2013), and such engagement involves the switch I and switch II regions of RhoA, and the β-strands connecting these two switches (Figure 2). The electron density is well defined for GTPγS and Mg^{2+} in the guanine nucleotide binding pocket of RhoA. The binding mode of Rac1•GTPγS to the PH domain of p190 is analogous to that between RhoA•GTPγS and p190-PH. Here again, the β 5, β6 and β7 strands of the PH domain from p190 interact directly with the switch I and switch II regions of Rac1. The two PH domains in these structures are almost identical. Cα atoms from these two p190-PH structures overlap with a root mean square (rms) deviation of 0.9 Å. However, significant movements of the C-terminal β-sheet, especially within the loop connecting β6 and β7 (residues 1157–1164), are observed when bound to different GTPases (Figure S6). The changes in Cα positions in this area range between 1 to 4 Å. The structure of RhoA or Rac1 in the complex is almost identical to that of RhoA or Rac1 bound to GTPγS alone, with a rms deviation of 0.5 Å for all Cα atoms.

3.3. The PH:GTPase interface

The surface on the PH domain of p190 that interacts with activated RhoA and Rac1 can be subdivided into three conjoining areas (Figure 3). Most of the major interactions between p190-PH and RhoA or Rac1 involve residues from the “Center-core site” (Figure 3B), including hydrophobic residues Ile-1142 from β5, Phe-1154 and Ile-1156 from β6, and Met-1165 from β7 of p190-PH. Arg-1144 from β5 of p190-PH extends over towards the GTPase, forming hydrogen bonds with the switch I region of RhoA or Rac1. Residues from RhoA or Rac1 making contacts with the Center-core site of p190-PH are highly conserved between the two proteins. They include Val-38, Phe-39 and Glu-40 from switch I of RhoA, two leucine residues (Leu-69 and Leu-72) from switch II of RhoA, as well as a tryptophan residue (Trp-58) from the β3 strand of RhoA preceding switch II. The corresponding set of residues in Rac1 include Val-36 and Phe-37 from switch I, two leucine residues (Leu-67 and Leu-70) from switch II, and Trp-56 from β3. However, glutatmate-40 in RhoA, whose side chain forms two salt bridges with the extending side chain of Arg-1144 from p190-PH, is replaced by an aspartic acid in Rac1. Although still negatively charged, the shorter side

chain of Asp-38 in Rac1 is not within hydrogen bonding distance of Arg-1144 from p190-PH. Rather, Arg-1144 forms one hydrogen bond with the main chain carbonyl group of Phe-37 from Rac1. As expected, mutations at the Center-core site on p190-PH resulted in lower binding affinity between the PH domain and activated RhoA (Medina et al., 2013); similar results for activated Rac1 are presented in subsequent results.

Flanking the Center-core site at the PH:GTPase interface are the “top site” (Figure 3A) and the “bottom site” (Figure 3C). Residues from the β6-β7 loop of p190-PH, and the switch II region of RhoA or Rac1 make up the interface at the top site, whereas the bottom site is dominated by the β5-β6 loop of p190-PH and the β2-β3 region of the GTPases. A closer look at these two sites reveals that activated RhoA makes more close contacts with the PH domain of p190 than activated Rac1. The most noticeable contact includes Asn-41 in RhoA, which forms two hydrogen bonds with main chain atoms of p190-PH (Figure 3C). This interaction is not observed between activated Rac1 and p190-PH, even though the asparagine is conserved between RhoA and Rac1.

3.4. The PH domain of p190RhoGEF interacts with RhoA more extensively than with Rac1

The interface between p190-PH and RhoA•GTPγS is very similar to that between p190-PH and activated Rac1. However, as shown earlier, the binding affinity between the PH domain of p190 and activated RhoA is at least 10 fold higher than that towards activated Rac1 (Figure 1). RhoA and Rac1 share high sequence similarity, especially for those residues that contact p190-PH (Figure 3D). However, when comparing the calculated electrostatic surface potentials of RhoA and Rac1, the surface on RhoA that is facing p190-PH in the structure is more negatively charged than that from Rac1 (Chen et al., 2010b). The β5-β6-β7 segment that contacts activated RhoA or Rac1 in p190-PH is notably electropositive (Figure S7), and complements the electronegative surface of RhoA better than Rac1; this raises the possibility that electrostatic attraction favors formation of a tighter complex between activated RhoA and the PH domain of p190. The overall structures of RhoA and Rac1 are very similar, with a rms deviation of 0.7 Å for all of the Cα atoms. A slight shift of the p190 PH domain can be observed when the two complex structures are superimposed based on coordinates of the small GTPases (Figure 4A, B). In the structure of p190-PH:Rac1, the PH domain is shifted slightly away from the center of the interface. Although such a movement has very limited impact on the interactions between p190-PH and activated Rac1 at the Center-core site, it reduces the number of van der waals contacts and hydrogen bonds between p190-PH and the small GTPase at the top site as well as the bottom site (Figure 3A, 3C, Figure 4). Perhaps as a result of this, local conformational changes are observed at the top site within the β6-β7 loop of the PH domain (Figure S6). The interface between the PH domain of p190 and activated RhoA buries a solvent accessible surface area of about 610 $Å^2$, significantly more than the approximate 480 $Å^2$ buried between p190-PH and activated Rac1 (Figure 4C). This reduction of buried surface area could be a direct consequence of the shifting of the p190 PH domain. It is likely that the difference in electrostatic potentials of the binding surface, the change of position of p190-PH when interacting with different GTPases, and the change in position 40 of RhoA from a glutamic acid to an aspartic acid in Rac1, all contribute to the 10 fold reduction in apparent binding affinity of p190-PH towards activated Rac1 bound to GTPγS (Figure 1). This diffuse contribution became apparent from numerous mutations of

single amino acids that showed little effect on apparent affinity although predicted to provide different interactions between p190-PH and RhoA or Rac1. For example, a triple mutation was designed to make RhoA look more like Rac1; amino acids E40, V43 and A56 of RhoA were altered to the corresponding amino acids (D, S and G) of Rac1, respectively. All three mutations combined resulted in only a 2-fold reduction in affinity of RhoA to p190-PH (Figure 5, Figure S8).

3.5. Activated RhoA and Rac1 facilitate stimulation of RhoA by p190RhoGEF in a membrane-delimited system

Previous reports showed that activated RhoA could bind to the PH domain of Lbc RhoGEFs (Chen et al., 2010b; Medina et al., 2013) and that this association could stimulate the ability of PRG to act on RhoA•GDP when both activated RhoA and substrate were localized to phospholipid vesicles (Medina et al., 2013). This same system was used to test the hypothesis that activated RhoA and Rac1 would similarly facilitate stimulation of p190RhoGEF.

In Figure 6, the exchange activity of added RhoGEF is measured by the increased dissociation of mant-GDP from RhoA that is sequestered to phospholipid vesicles. The soluble DHPH domain of p190 increases the basal exchange of nucleotide from RhoA (Figure 6A); there was no apparent difference in this rate of exchange in the presence of inactive Rac1 also bound to the vesicles. However, a robust increase in the rate of exchange was observed when the active Rac1 was bound to the vesicles. This result is due to the localization, as the increase was not observed if the activated Rac1 lacked the c-terminal 6-His tag (Figure S9A). Similar results were seen with RhoA; only the active form of RhoA that was localized to the vesicles stimulated the nucleotide exchange activity of p190-DHPH on its membrane associated substrate (Figure 6B, S9B). The larger effect of activated RhoA could be explained by its higher binding affinity for p190-PH (Figure 1).

The dependence of this facilitation on binding of the activated GTPases to the PH domain of p190RhoGEF was examined by mutations that attenuate this binding. A crystal structure of the binding interaction between the PRG PH domain and RhoA•GTPγS showed that binding occurred between the switch regions of RhoA and a highly conserved hydrophobic patch in the PH domain of the RhoGEF (Chen et al., 2010b; Medina et al., 2013). The structures shown herein confirm the conservation of these binding sites across the family of Lbc RhoGEFs and help validate mutations previously shown in the PH domains of various members that abolished binding to activated RhoA (Medina et al., 2013). Since the PH domain of p190RhoGEF binds to both RhoA and Rac1, the previous defined double mutation (F1154A and I1156A) that was shown to disrupt binding to RhoA was tested for its ability to disrupt binding to Rac1. In a pulldown assay similar to Figure 1, such mutations in the PH domain of p190 attenuated binding to activated Rac1 as well as activated RhoA (Figure 7A).

These mutations in the context of the DHPH domains of p190 were used to look for attenuation of regulation in the membrane delimited assays. In this experiment, guanine nucleotide exchange was assessed by the increase of fluorescence of mant-GDP bound to RhoA in place of dissociated GDP. While the mutations did not affect the basal exchange

activity of p190RhoGEF, the increased activity of the RhoGEF in the presence of activated Rac1 localized to vesicle membranes was clearly eliminated by the mutations (Figure 7B). Similar results were seen when activated RhoA was localized to the vesicle membrane, in which stimulation of the RhoGEF activity was abolished by the mutations (Figure 7C). These results demonstrate that stimulation of the p190 DHPH domains in this context is due to binding between the activated GTPases and the PH domain observed in the structures reported here.

3.6. Stimulation of other Lbc RhoGEFs by activated Rac1

The ability of Rac1 to facilitate activity of p190RhoGEF on membrane substrates in spite of its relatively low affinity, and recognition of the same binding site as activated RhoA, raised the question of whether this interaction is unique to p190RhoGEF, or also a property of other Lbc RhoGEFs. Since pulldown assays with activated Rac1 did not detect interactions with the PH domains of various Lbc RhoGEFs (PRG, LARG, and GEFH1), the DHPH domains of various Lbc family RhoGEFs were further tested with the more sensitive phospholipid vesicle assays. In these assays, where activated Rac1 was localized to the lipid membrane along with substrate, we detected a modest ability of Rac1 to increase the initial exchange rate of LARG (1.7 fold), AKAP-Lbc (2.4 fold) and p114RhoGEF (2.5 fold) (Figure 8). However, these stimulations were small compared to the more robust action on p190RhoGEF (7.9 fold). In this respect, the lack of detection of binding by pulldowns correlates well with reduced effectiveness in the functional assay.

4. Discussion

Recently, we characterized the interaction of the PH domains of various Lbc family RhoGEFs with the activated small GTPase, RhoA, and demonstrated that this could serve as a positive feedback mechanism for robust activation of RhoA (Medina et al., 2013). In the current study, we found that the PH domain of one of these, p190RhoGEF, could also bind to activated Rac1, suggesting a mechanism for crosstalk between the regulation evoked by these two GTPases.

To better understand the binding between p190-PH and its two GTPase partners, we successfully generated crystal structures of the isolated PH domain of p190RhoGEF in complexes with either activated RhoA or Rac1. The structure of p190-PH bound to RhoA•GTPγS largely mimics the interaction of activated RhoA with the PH domain of PRG (Chen et al., 2010b) and verifies the conservation of this binding motif predicted for the Lbc RhoGEF family (Aittaleb et al., 2009; Medina et al., 2013). Our second structure reveals the unique interaction of p190-PH with activated Rac1. It shows a similar binding pattern between the switch regions on the GTPase and the same patch of mostly hydrophobic surface area located on the C-terminal beta-sheets on the PH domain that interact with activated RhoA. This common binding interface was verified by mutagenesis of key amino acid residues on the PH domain of p190RhoGEF, which abolished binding of the PH domain to both activated RhoA and Rac1 as well as the ability of these GTPases to stimulate the activity of p190RhoGEF on membrane delimited RhoA.

Localization of RhoGEFs to the plasma membrane is a proposed mechanism for regulation of these proteins (Rossman et al., 2005; Viaud et al., 2012). We have shown that such a mechanism can utilize the endogenous activity of Lbc RhoGEFs to activate membrane delimited RhoA (Medina et al., 2013) and mediate hormone regulation of the GTPase via the heterotrimeric G12/13 proteins (Carter et al., 2014). This mechanism should be viable for the similar interaction of the PH domain of p190RhoGEF with activated RhoA. However, effective regulation becomes less obvious considering the weaker association of Rac1•GTPγS with p190-PH, as evinced from both biophysical and biochemical techniques. We utilized an in-vitro signaling system (Medina et al., 2013) to verify that pre-activated RhoA bound to the vesicles would increase the exchange activity of p190RhoGEF on membrane associated RhoA. The ability of activated Rac1 to function similarly demonstrates that this low affinity interaction is also sufficient for membrane localization. Nevertheless, the smaller improvement in the initial exchange rate seen with Rac1 versus RhoA presumably reflects this difference in binding affinities and a less robust response. The high homology and structural similarity of Cdc42 to Rac1 suggested that it may also show an interaction with p190-PH. While binding between p190-PH and activated Cdc42 was never observed in dot blot or pull-down assays, its ability to interact with p190-PH was observed in the more sensitive vesicle activity assay (Figure S10).

Competition binding data provided an estimated affinity for interaction of activated Rac for p190-PH in the range of 20 μM, fully 10-fold less than binding between p190-PH and RhoA•GTPγS. Is this relevant in the cellular environment? Two observations support the potential of this low affinity interaction for effective action in cells. First, the PH domain of p115RhoGEF was also not observed to bind to activated RhoA in a pull-down assay, but could be shown to inhibit regulation by activated Rho in cells by overexpression (Medina et al., 2013). Second, point mutations at the Center-core site that disrupted binding of activated RhoA to the PH domain severely attenuated the ability of p115RhoGEF to activate RhoA by overexpression. Recent experiments have estimated the affinity of p115-PH:RhoA•GTPγS to be in the range of 50 μM (see Figure 1 in Chen et al., Data in Brief, submitted), lower than the observed affinity of p190-PH:Rac1•GTPγS reported here. Finally, the low affinities reported were measured in solution. Once the RhoGEF is localized to the 2-dimensional space of a membrane surface along with its substrate, effective concentrations become much greater, both for substrate turnover and potential interaction of other membrane components with the RhoGEF. In support of the latter hypothesis, a wide range of binding affinities has also been reported between the PH domains of some members in the Dbl family of RhoGEFs and phospholipids, especially phosphoinositides (Viaud et al., 2012). In this scenario, while clear roles have been shown for specific RhoGEFs, the relatively low affinities of many domains towards phospholipids suggest that these interactions alone are insufficient for membrane localization (Rossman et al., 2005). Both reviews propose that low affinity interactions may facilitate other mechanisms for binding of these proteins to membranes. Such a mechanism may also apply to potential regulation of p190RhoGEF by Rac1.

Whereas binding of activated RhoA to the PH domains of the RhoGEFs is proposed to mediate positive feedback regulation (Chen et al., 2010b; Medina et al., 2013), the sequestration of p190RhoGEF by activated Rac1 reveals a novel putative physiological role,

that is to utilize Rac1 to directly drive regulation of RhoA. The low affinity for Rac1 may then suggest that this putative regulation requires either very robust action by Rac1 prior to initiating regulation of RhoA, or the action of a partner that facilitates the ability of Rac1 to localize p190RhoGEF. The relatively weak interaction of p190-PH for phosphoinositides (Miller et al., 2013) may offer a mechanism for the latter facilitory role. Prior studies on Dbs, a RhoGEF that activates RhoA, support this hypothesis. The PH domain of this GEF can bind to phosphoinositides (Snyder et al., 2001) and activated Rac1 (Cheng et al., 2004); further, coexpression of activated Rac1 and Dbs in NIH3T3 cells enhanced the ability of overexpressed Dbs to stimulate activation of RhoA and cause foci formation (Cheng et al., 2004).

What is the physiological role of Rac binding to p190RhoGEF? Many RhoGEFs play roles in various aspects of cellular motility, such as adhesion, contractility, and tail retraction (Chikumi et al., 2002; Dubash et al., 2007; Francis et al., 2006; Iwanicki et al., 2008; Lim et al., 2008; Miller et al., 2012; Zhai et al., 2003). An interesting feature of p190RhoGEF is its potential contribution to cellular matrix attachment and localization to the focal adhesions involved (Miller et al., 2012). A current model for adhesion predicts a major role for activation of Rac in the formation process with an increasingly contribution of RhoA in maturation and strengthening of the focal adhesion (Guilluy et al., 2011; Guo et al., 2006). Binding of p190RhoGEF to focal adhesion kinase (FAK) has been proposed as a mechanism for localization of the GEF to foci (Zhai et al., 2003). The data reported herein suggest that activated Rac could be a recruitment mechanism or synergize with the binding to FAK to keep p190RhoGEF at the focal adhesion and drive effective catalysis of RhoA at the same site. This would then coordinate a switch to the stabilizing action of RhoA, which could then enhance its own function through its positive feedback mechanism. An interesting test of this hypothesis would be the use of p190RhoGEF mutants, where the binding to Rac1 and RhoA were selectively dissected; unfortunately, the residues on the PH domain used for interaction with the GTPases are essentially the same and mutation of core residues eliminates binding to both GTPases (Figures 1, 7). Similarly, attempts to exploit differences between residues in the GTPases produced only modest changes (Figure S8).

The physiological importance of the interaction of activated Rac1 and the p190 PH domain may be indicated from an examination of the effect of Rac1 on other Lbc RhoGEFs. The seven members of this family can be split into two groups characterized by their relative homology among the DHPH domains and the absence (p190RhoGEF, p114RhoGEF, AKAP-Lbc, GEFH1) or presence of an RH domain (p115RhoGEF, LARG, PRG) (Medina et al., 2013; Sternweis et al., 2007). All five of the Lbc RhoGEFs that were tested for activation of RhoA in the vesicle assay showed an increased activity in the presence of membrane associated Rac1•GTPγS (Figure 8). While the extent of activation increases with similarity to p190RhoGEF, the latter clearly stands out, suggesting that this is a specialized function of the RhoGEF. A second indication of specialized function is that the order of potency for binding of RhoA to the same site on Lbc RhoGEFs is completely different; indeed, p190RhoGEF ranks second to PRG in potency for binding activated RhoA (see Figure 1 in Chen et al., Data in Brief, submitted). The RhoGEFs with an RH domain and specialized responsiveness to signaling via the heterotrimeric G12/13 proteins show the least effect of Rac1; this emphasizes the divergence in function of these homologous RhoGEFs.

The relatively smaller effects of Rac1 on related Lbc RhoGEFs relative to RhoA raises the question of whether this merely reflects the residual interaction of proteins with highly conserved interacting surfaces, RhoA versus Rac1, with the conserved hydrophobic region of Lbc PH domains. If this is largely true, the ability of Rac1 to interact more effectively with p190RhoGEF may have evolved from this motif to serve a specialized crosstalk function.

Supplementary Material

Refer to Web version on PubMed Central for supplementary material.

Acknowledgments

We thank Jana Hadas and Thomas Scheuermann for technical assistance, and the staff of APS for assistance with data collection. This work was supported by National Institute of Health Grants GM31954 (to P. C. S.), and the Alfred and Mabel Gilman Chair in Molecular Pharmacology (P. C. S.). Some results shown in this report are derived from work performed at Argonne National Laboratory, Structural Biology Center at APS. Argonne is operated by U Chicago Argonne, LLC, for the U.S. Department of Energy, Office of Biological and Environmental Research under Contract DE-AC02-06CH11357.

Abbreviations

RhoGEF	Rho guanine nucleotide exchange factors
RhoGAP	GTPase-activating proteins
DH	Dbl homology
PH	pleckstrin homology
PRG	PDZRhoGEF
TEV	Tobacco Etch Virus
His_6	hexahistidine peptide
GST	glutathione S-transferase
ITC	isothermal titration calorimetry
AUC	analytical ultracentrifugation

References

Adams PD, Afonine PV, Bunkoczi G, Chen VB, Davis IW, Echols N, Headd JJ, Hung LW, Kapral GJ, Grosse-Kunstleve RW, et al. PHENIX: a comprehensive Python-based system for macromolecular structure solution. Acta Crystallogr D Biol Crystallogr. 2010; 66:213–221. [PubMed: 20124702]

Aittaleb M, Gao G, Evelyn CR, Neubig RR, Tesmer JJG. A conserved hydrophobic surface of the LARG pleckstrin homology domain is critical for RhoA activation in cells. Cellular Signalling. 2009; 21:1569–1578. [PubMed: 19560536]

Berman HM, Westbrook J, Feng Z, Gilliland G, Bhat TN, Weissig H, Shindyalov IN, Bourne PE. The Protein Data Bank. Nucleic Acids Res. 2000; 28:235–242. [PubMed: 10592235]

Bos JL, Rehmann H, Wittinghofer A. GEFs and GAPs: critical elements in the control of small G proteins. Cell. 2007; 129:865–877. [PubMed: 17540168]

Brautigam, CA. Chapter Five - Calculations and Publication-Quality Illustrations for Analytical Ultracentrifugation Data. In: James, LC., editor. Methods in Enzymology. Academic Press; 2015. p. 109-133.

Cañete-Soler R, Wu J, Zhai J, Shamim M, Schlaepfer WW. p190RhoGEF Binds to a Destabilizing Element in the 3′ Untranslated Region of Light Neurofilament Subunit mRNA and Alters the Stability of the Transcript. Journal of Biological Chemistry. 2001; 276:32046–32050. [PubMed: 11435431]

Carter AM, Gutowski S, Sternweis PC. Regulated Localization Is Sufficient for Hormonal Control of Regulator of G Protein Signaling Homology Rho Guanine Nucleotide Exchange Factors (RH-RhoGEFs). Journal of Biological Chemistry. 2014; 289:19737–19746. [PubMed: 24855647]

Chen VB, Arendall WB, Headd JJ 3rd, Keedy DA, Immormino RM, Kapral GJ, Murray LW, Richardson JS, Richardson DC. MolProbity: all-atom structure validation for macromolecular crystallography. Acta Crystallogr D Biol Crystallogr. 2010a; 66:12–21. [PubMed: 20057044]

Chen Z, Gutowski S, Sternweis PC. Crystal Structures of the PH Domains from Lbc Family of RhoGEFs bound to Activated RhoA GTPase. Data in Brief, *Submitted*.

Chen Z, Medina F, Liu M-Y, Thomas C, Sprang SR, Sternweis PC. Activated RhoA Binds to the Pleckstrin Homology (PH) Domain of PDZ-RhoGEF, a Potential Site for Autoregulation. Journal of Biological Chemistry. 2010b; 285:21070–21081. [PubMed: 20430886]

Chen Z, Singer WD, Danesh SM, Sternweis PC, Sprang SR. Recognition of the activated states of Galpha13 by the rgRGS domain of PDZRhoGEF. Structure. 2008; 16:1532–1543. [PubMed: 18940608]

Cheng L, Mahon GM, Kostenko EV, Whitehead IP. Pleckstrin homology domain-mediated activation of the rho-specific guanine nucleotide exchange factor Dbs by Rac1. J Biol Chem. 2004; 279:12786–12793. [PubMed: 14701795]

Cherfils J, Zeghouf M. Regulation of small GTPases by GEFs, GAPs, and GDIs. Physiol Rev. 2013; 93:269–309. [PubMed: 23303910]

Chikumi H, Fukuhara S, Gutkind JS. Regulation of G protein-linked guanine nucleotide exchange factors for Rho, PDZ-RhoGEF, and LARG by tyrosine phosphorylation: evidence of a role for focal adhesion kinase. J Biol Chem. 2002; 277:12463–12473. [PubMed: 11799111]

Dam J, Schuck P. Sedimentation Velocity Analysis of Heterogeneous Protein-Protein Interactions: Sedimentation Coefficient Distributions c(s) and Asymptotic Boundary Profiles from Gilbert-Jenkins Theory. Biophys J. 2005; 89:651–666. [PubMed: 15863474]

DeLano WL. The PyMOL Molecular Graphics System. 2002

Dubash AD, Wennerberg K, Garcia-Mata R, Menold MM, Arthur WT, Burridge K. A novel role for Lsc/p115 RhoGEF and LARG in regulating RhoA activity downstream of adhesion to fibronectin. J Cell Sci. 2007; 120:3989–3998. [PubMed: 17971419]

Emsley P, Lohkamp B, Scott WG, Cowtan K. Features and development of Coot. Acta Crystallogr D Biol Crystallogr. 2010; 66:486–501. [PubMed: 20383002]

Etienne-Manneville S, Hall A. Rho GTPases in cell biology. Nature. 2002; 420:629–635. [PubMed: 12478284]

Francis SA, Shen X, Young JB, Kaul P, Lerner DJ. Rho GEF Lsc is required for normal polarization, migration, and adhesion of formyl-peptide–stimulated neutrophils. Blood. 2006; 107:1627–1635. [PubMed: 16263795]

García De La Torre J, Huertas ML, Carrasco B. Calculation of hydrodynamic properties of globular proteins from their atomic-level structure. Biophys J. 2000; 78:719–730. [PubMed: 10653785]

Gebbink MFBG, Kranenburg O, Poland M, vanHorck FPG, Houssa B, Moolenaar WH. Identification of a novel, putative Rho-specific GDP/GTP exchange factor and a RhoA-binding protein: Control of neuronal morphology. Journal of Cell Biology. 1997; 137:1603–1613. [PubMed: 9199174]

Guilluy C, Garcia-Mata R, Burridge K. Rho protein crosstalk: another social network? Trends Cell Biol. 2011; 21:718–726. [PubMed: 21924908]

Guo F, Debidda M, Yang L, Williams DA, Zheng Y. Genetic deletion of Rac1 GTPase reveals its critical role in actin stress fiber formation and focal adhesion complex assembly. J Biol Chem. 2006; 281:18652–18659. [PubMed: 16698790]

Iwanicki MP, Vomastek T, Tilghman RW, Martin KH, Banerjee J, Wedegaertner PB, Parsons JT. FAK, PDZ-RhoGEF and ROCKII cooperate to regulate adhesion movement and trailing-edge retraction in fibroblasts. Journal of Cell Science. 2008; 121:895–905. [PubMed: 18303050]

Jaiswal M, Gremer L, Dvorsky R, Haeusler LC, Cirstea IC, Uhlenbrock K, Ahmadian MR. Mechanistic Insights into Specificity, Activity, and Regulatory Elements of the Regulator of G-protein Signaling (RGS)-containing Rho-specific Guanine Nucleotide Exchange Factors (GEFs) p115, PDZ-RhoGEF (PRG), and Leukemia-associated RhoGEF (LARG). Journal of Biological Chemistry. 2011; 286:18202–18212. [PubMed: 21454492]

Keller S, Vargas C, Zhao H, Piszczek G, Brautigam CA, Schuck P. High-Precision Isothermal Titration Calorimetry with Automated Peak-Shape Analysis. Analytical Chemistry. 2012; 84:5066–5073. [PubMed: 22530732]

Lim Y, Lim ST, Tomar A, Gardel M, Bernard-Trifilo JA, Chen XL, Uryu SA, Canete-Soler R, Zhai J, Lin H, et al. PyK2 and FAK connections to p190Rho guanine nucleotide exchange factor regulate RhoA activity, focal adhesion formation, and cell motility. J Cell Biol. 2008; 180:187–203. [PubMed: 18195107]

Lin H, Zhai J, Schlaepfer WW. RNA-binding protein is involved in aggregation of light neurofilament protein and is implicated in the pathogenesis of motor neuron degeneration. Human Molecular Genetics. 2005; 14:3643–3659. [PubMed: 16236762]

McCoy AJ, Grosse-Kunstleve RW, Adams PD, Winn MD, Storoni LC, Read RJ. Phaser crystallographic software. Journal of Applied Crystallography. 2007; 40:658–674. [PubMed: 19461840]

Medina F, Carter AM, Dada O, Gutowski S, Hadas J, Chen Z, Sternweis PC. Activated RhoA Is a Positive Feedback Regulator of the Lbc Family of Rho Guanine Nucleotide Exchange Factor Proteins. Journal of Biological Chemistry. 2013; 288:11325–11333. [PubMed: 23493395]

Meyer D, Liu A, Margolis B. Interaction of c-Jun Amino-terminal Kinase Interacting Protein-1 with p190 rhoGEF and Its Localization in Differentiated Neurons. Journal of Biological Chemistry. 1999; 274:35113–35118. [PubMed: 10574993]

Miller NLG, Lawson C, Chen XL, Lim ST, Schlaepfer DD. Rgnef (p190RhoGEF) Knockout Inhibits RhoA Activity, Focal Adhesion Establishment, and Cell Motility Downstream of Integrins. PLoS One. 2012; 7:e37830. [PubMed: 22649559]

Miller NLG, Lawson C, Kleinschmidt EG, Tancioni I, Uryu S, Schlaepfer DD. A non-canonical role for Rgnef in promoting integrin-stimulated focal adhesion kinase activation. Journal of Cell Science. 2013; 126:5074–5085. [PubMed: 24006257]

Otwinowski Z, Minor W. Processing of X-ray Diffraction Data Collected in Oscillation Mode. Methods in Enzymology. 1997; 276:307–326.

Ramachandran GN, Sassiekharan V. Conformation of polypeptides and proteins. Advances in Protein Chemistry. 1968; 28:283–437.

Rossman KL, Der CJ, Sondek J. GEF means go: turning on RHO GTPases with guanine nucleotide-exchange factors. Nat Rev Mol Cell Biol. 2005; 6:167–180. [PubMed: 15688002]

Schaefer A, Reinhard NR, Hordijk PL. Toward understanding RhoGTPase specificity: structure, function and local activation. Small GTPases. 2014; 5:6. [PubMed: 25483298]

Schuck P. Size-distribution analysis of macromolecules by sedimentation velocity ultracentrifugation and lamm equation modeling. Biophys J. 2000; 78:1606–1619. [PubMed: 10692345]

Schuck P. On the analysis of protein self-association by sedimentation velocity analytical ultracentrifugation. Analytical Biochemistry. 2003; 320:104–124. [PubMed: 12895474]

Snyder JT, Rossman KL, Baumeister MA, Pruitt WM, Siderovski DP, Der CJ, Lemmon MA, Sondek J. Quantitative analysis of the effect of phosphoinositide interactions on the function of Dbl family proteins. J Biol Chem. 2001; 276:45868–45875. [PubMed: 11577097]

Sternweis PC, Carter AM, Chen Z, Danesh SM, Hsiung YF, Singer WD. Regulation of Rho guanine nucleotide exchange factors by G proteins. Adv Protein Chem. 2007; 74:189–228. [PubMed: 17854659]

van Horck FPG, Ahmadian MR, Haeusler LC, Moolenaar WH, Kranenburg O. Characterization of p190RhoGEF, A RhoA-specific Guanine Nucleotide Exchange Factor That Interacts with Microtubules. Journal of Biological Chemistry. 2001; 276:4948–4956. [PubMed: 11058585]

Viaud J, Gaits-Iacovoni F, Payrastre B. Regulation of the DH-PH tandem of guanine nucleotide exchange factor for Rho GTPases by phosphoinositides. Adv Biol Regul. 2012; 52:303–314. [PubMed: 22781744]

Yu HG, Nam JO, Miller NL, Tanjoni I, Walsh C, Shi L, Kim L, Chen XL, Tomar A, Lim ST, et al. p190RhoGEF (Rgnef) promotes colon carcinoma tumor progression via interaction with focal adhesion kinase. Cancer Res. 2011; 71:360–370. [PubMed: 21224360]

Zhai J, Lin H, Nie Z, Wu J, Canete-Soler R, Schlaepfer WW, Schlaepfer DD. Direct interaction of focal adhesion kinase with p190RhoGEF. J Biol Chem. 2003; 278:24865–24873. [PubMed: 12702722]

Zhai J, Lin H, Shamim M, Schlaepfer WW, Cañete-Soler R. Identification of a Novel Interaction of 14-3-3 with p190RhoGEF. Journal of Biological Chemistry. 2001; 276:41318–41324. [PubMed: 11533041]

Zhao H, Piszczek G, Schuck P. SEDPHAT – A platform for global ITC analysis and global multi-method analysis of molecular interactions. Methods. 2015; 76:137–148. [PubMed: 25477226]

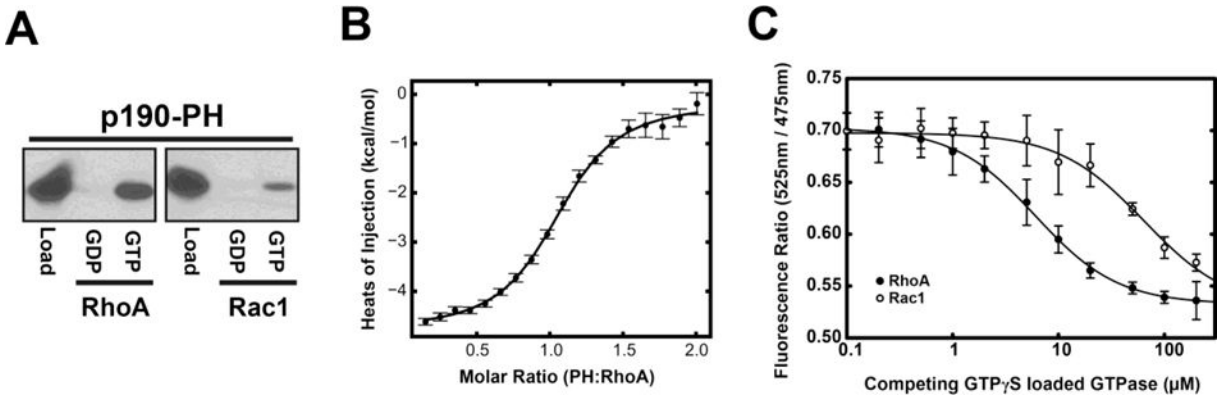

Figure 1. The PH domain from p190RhoGEF binds activated RhoA and Rac1

A. Purified His_6-p190 PH domains (12 pmol) were incubated with immobilized basal (GDP) or active (GTP) forms of GST-RhoA (80 pmol) or GST-Rac1 (80 pmol). PH domains that bound to the resin were eluted, separated by SDS-PAGE and visualized by immunoblotting. B. Measurement of the binding affinity between the p190-PH and RhoA•GTPγS by isothermal titration calorimetry. C. The ability of non-tagged RhoA•GTPγS and Rac1•GTPγS to bind to p190PH was measured by competition using the FRET signal produced by association of 2 μM YFP-RhoA•GTPγS with 2 μM CFP-p190-PH. Sections 2.4, 2.5, and 2.11 provide further details. Error bars in panel B represent the uncertainty of each individual integrated isotherm peak assigned by the program, NITPIC; error bars in panel C are the standard deviation of the averaged data from 3 independent experiments.

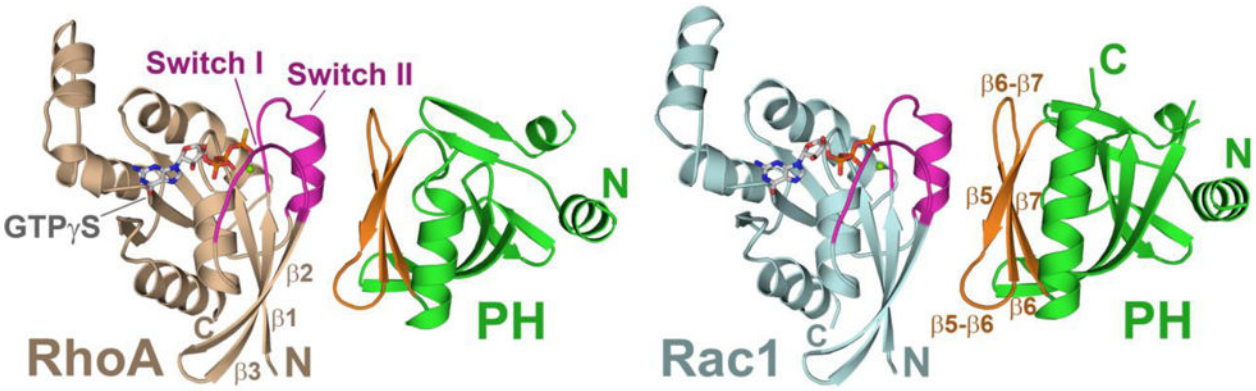

Figure 2. Structures of the p190 PH domain in complexes with activated GTPases

Ribbon diagrams depicting tertiary structures of p190-PH in a complex with RhoA•GTPγS (left) or Rac1•GTPγS (right). p190-PH is colored green, with the C-terminal layer of β-strands colored orange. RhoA is colored wheat, with switch regions colored purple. Rac1 is colored cyan, with switch regions colored purple. GTPγS is depicted as a stick model and colored as follows: oxygen, nitrogen, carbon and phosphorous atoms are colored red, blue, grey, and yellow, respectively. Magnesium is shown as a green ball.

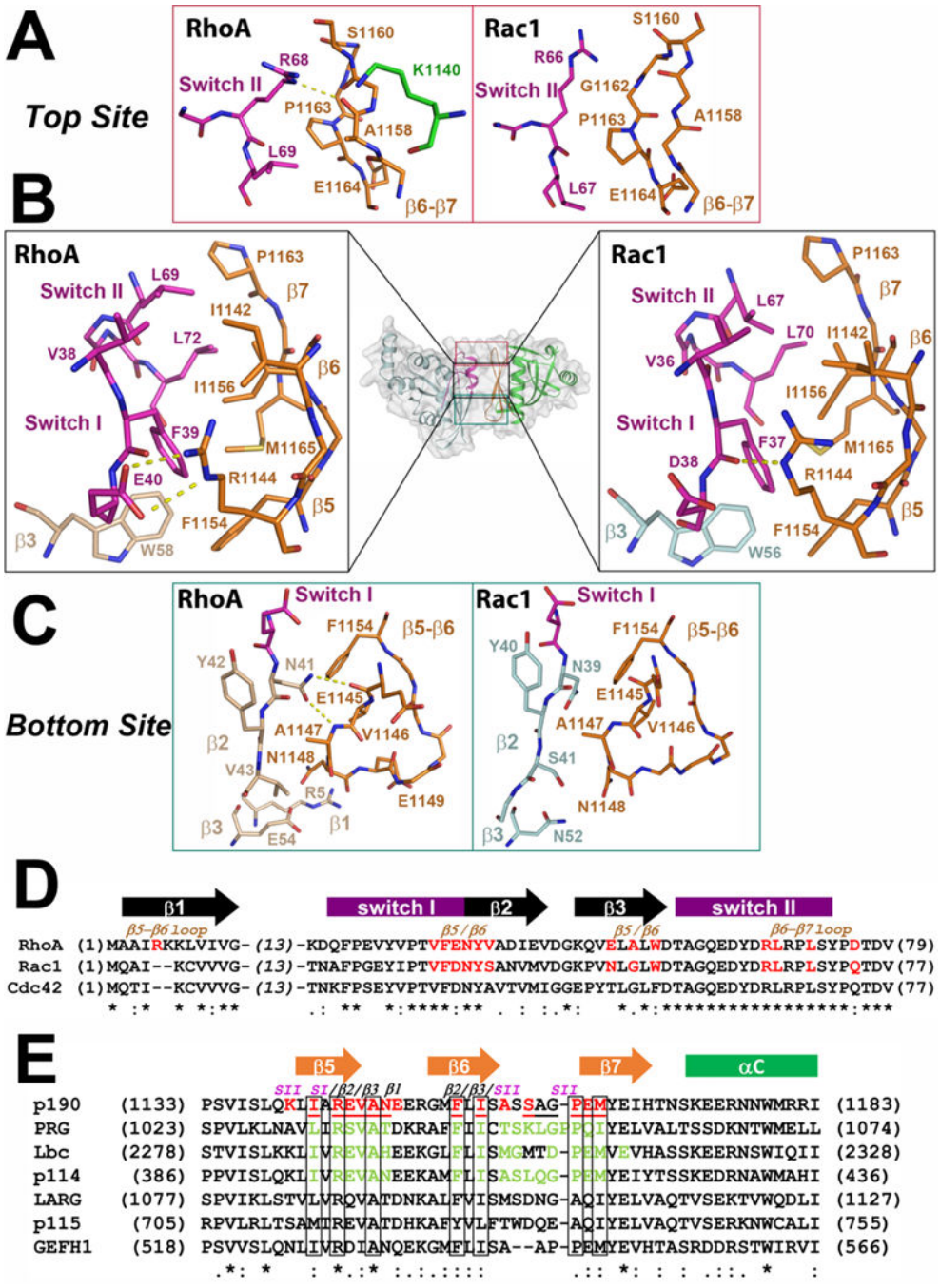

Figure 3. Comparison between the interfaces of PH•RhoA and PH•Rac1

The overall structure of the complexes is depicted as ribbon diagrams of the p190-PH•Rac1 structure at the center of the figure; this uses the same coloring scheme as in Figure 2. The top three panels subdivide the interfaces into three prominent parts, a top site (red boxes), a center core site (black boxes), and a bottom site (turquoise boxes). A. Side-by-side comparison of the top sites between p190-PH and activated RhoA (left) and activated Rac1 (right). Hydrogen bonds are drawn as dotted lines and colored yellow. Residues are labeled and color-coded as shown in Figure 2. B. The center core site between p190-PH and either

activated RhoA or Rac1. C. A side-by-side comparison of the bottom sites between p190-PH and activated RhoA (left) and activated Rac1 (right). D. Partial sequence alignment of Rho family small GTPases. The two flexible switch elements are indicated by purple blocks on top. Residues in RhoA or Rac1 that are involved in contacts with p190-PH are colored red. Corresponding secondary elements in p190-PH contacting these residues are labeled in italic and colored brown on top of the residues. E. Partial sequence alignment of the PH domains of Lbc RhoGEFs in the proposed contact regions for activated GTPases. Secondary structure has been assigned on the basis of the structure of p190-PH. Residues in p190-PH contacting RhoA are colored red. Residues in p190-PH contacting Rac1 are underlined. Residues from PRG-PH (Chen et at., 2010b), AKAP-Lbc-PH, and p114-PH (see Figures 2 and 3 in Chen et al., Data in Brief, submitted) that make contacts with activated RhoA in the PH:RhoA•GTPγS crystal structures are colored green. Residues that are highly conserved and contribute most to the interface between PH and activated GTPases are boxed. Corresponding secondary elements in activated GTPases (Rho or Rac1) contacting these residues are labeled in italic on top of the residues in the PH domains.

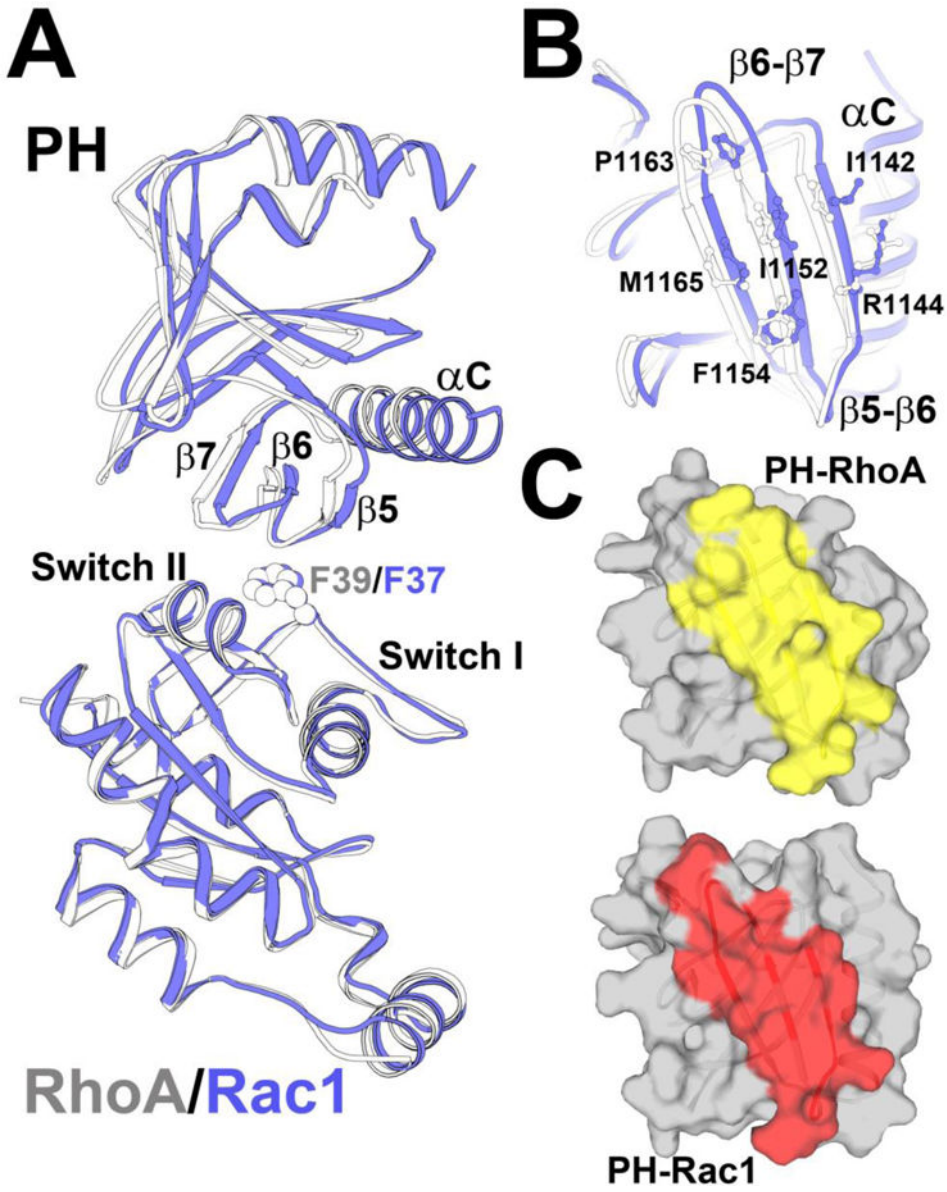

Figure 4. Slight repositioning of p190-PH when bound to different GTPases

A. The structure of the p190-PH•RhoA complex (white ribbons) is aligned against the structure of the p190-PH•Rac1 complex (blue ribbons). The alignment is based solely on coordinates from the GTPases, which highlights the altered positioning of the p190 PH domain when interacting with different GTPases. The highly conserved phenylalanine residues in switch I (Phe-39 in RhoA, or Phe-37 in Rac1) are drawn as ball-and-stick models. B. The different positioning of p190-PH is viewed from the perspective of the GTPase. A subset of residues from p190-PH contributing to the binding interface are depicted as ball-and-stick models and colored as in panel A. C. Surface representation of p190-PH with residues making contacts with RhoA or Rac1 colored yellow or red, respectively. The PH domain is oriented as in panel B.

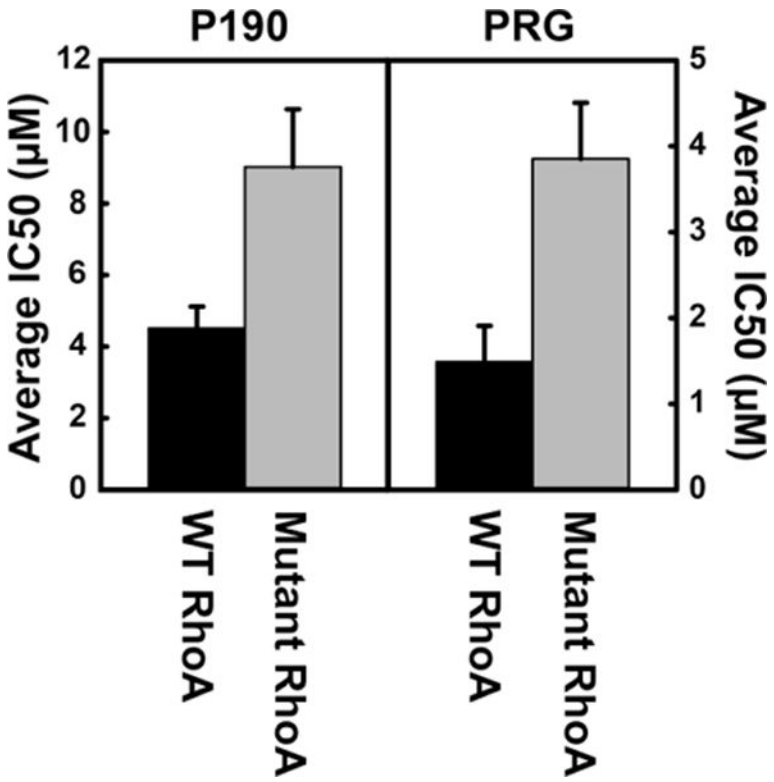

Figure 5. Mutations on RhoA reduce its ability to bind to the p190 PH domain

The relative ability of non-tagged wild-type RhoA•GTPγS or mutant (E40D/V43S/A56G) RhoA•GTPγS to bind to the p190 PH domain was measured by competition of the FRET produced by binding of 2 μM YFP-RhoA•GTPγS to 2 μM CFP-p190-PH (see Figure S8 for competition curves). The ability of both non-tagged wild-type and mutant RhoA•GTPγS to bind to PRG-PH was measured by competition of the FRET produced by binding of 1 μM YFP-RhoA•GTPγS to 1 μM CFP-PRG-PH. IC50 values were averaged from 3 separate titrations of each Rho; error bars are std dev. See section 2.1 for construction of sensors.

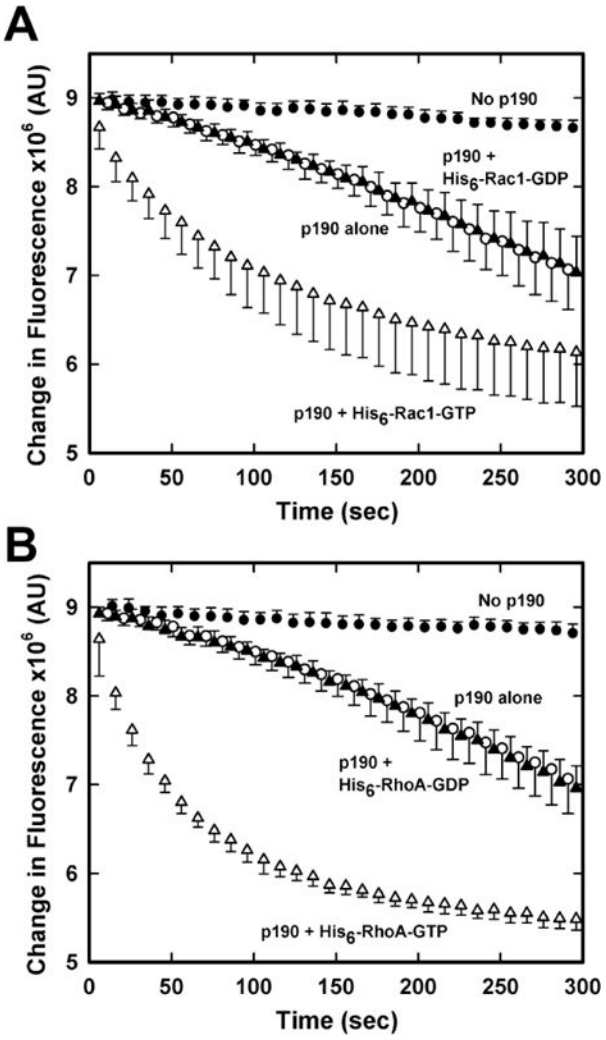

Figure 6. Only the active forms of RhoA and Rac1 enhance the nucleotide exchange activity of p190RhoGEF on RhoA associated with phospholipid vesicles

Nucleotide exchange assays were performed with phospholipid vesicles containing Ni-complexed lipids and 1 μM His_6-RhoA•mant-GDP as described in section 2.10. Nucleotide exchange was monitored by the decrease of fluorescence in mant-GDP as it dissociated from RhoA. A. Vesicles were supplemented with 100 nM His_6-Rac1•GDP (▲) or 100 nM His_6-Rac1•GTPγS (Δ) and reactions started with addition of 250 nM p190-DHPH (○,▲,Δ) as indicated. B. Vesicles were supplemented with 100 nM His_6-RhoA•GDP (▲) or 100 nM His_6-RhoA•GTPγS (Δ) and reactions started with addition of 250 nM p190-DHPH (○,▲,Δ) domains as indicated. Results are the average of three independent experiments (error bars are standard deviations).

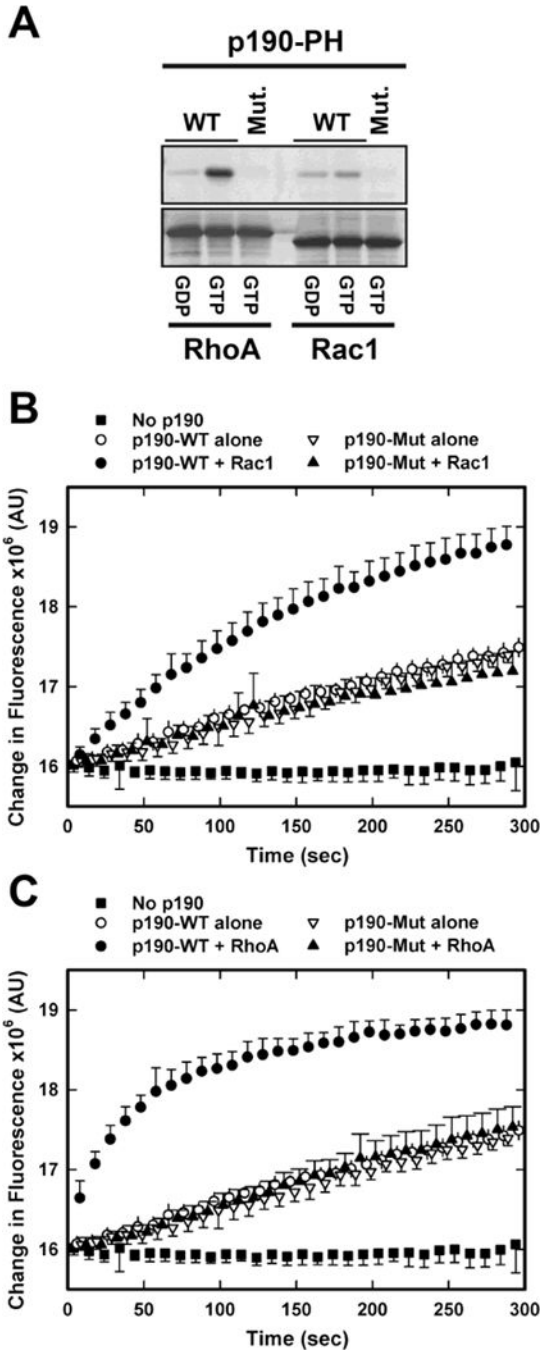

Figure 7. Mutations in p190-PH reduce its ability to bind to the active forms of RhoA and Rac1 and attenuate facilitation of p190RhoGEF activity on vesicle-delimited substrate

A. Purified p190-PH, either WT or p190-Mut (containing the mutations, F1154A, I1156A), were incubated with immobilized GST-RhoA or GST-Rac1 with either excess GDP or after preactivation with GTPγS, as indicated. PH domains bound to the immobilized GTPases were eluted, separated by SDS-PAGE, and visualized by silver staining. B. Nucleotide exchange assays were performed with phospholipid vesicles containing bound 1 μM His_6-RhoA•GDP. Assays included 2.5 μM free mant-GDP and nucleotide exchange was monitored by the increase in mant-GDP fluorescence as it bound to RhoA. Assays were

supplemented with 100 nM His_6-Rac1•GTPγS (●, ▲) as indicated and nucleotide exchange was initiated with addition of either 250 nM p190-DHPH-WT (○, ●) or 250 nM p190-DHPH-Mut (invertedΔ, ▲,), as indicated. C. Nucleotide exchange assays were performed as in B but with 100 nM His_6-RhoA•GTPγS (●, ▲). Results for panels B and C are the average of three independent experiments (error bars are standard deviations).

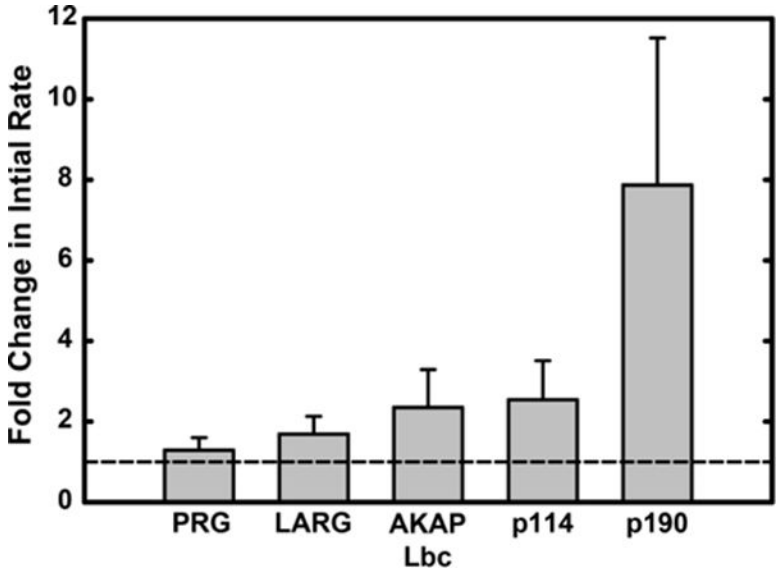

Figure 8. Stimulation of the initial rates of nucleotide exchange by various Lbc family RhoGEFs by pre-activated Rac1 on phospholipid vesicles

Nucleotide exchange assays were assessed by dissociation of bound mant-GDP from vesicle delimited RhoA as in Figure 6. Assays were initiated with the DHPH domains of PRG (25nM), LARG (25nM), AKAP-Lbc (100nM), p114RhoGEF (500nM), and p190RhoGEF (250nM). The initial exchange rates stimulated by addition of the RhoGEFs either in the absence or presence of 1 μM His_6-Rac1•GTPγS were determined; the fold increases in stimulation by activated Rac1 over the RhoGEF alone are shown. Data from three separate experiments were normalized by total signal and averaged; error bars are the standard deviation for each condition.

Table 1

	PH : RhoA	PH-*linker*-Rac1
Data Collection		
Source	APS SBC 19ID	APS SBC 19ID
Wavelength (Å)	0.9792	0.9793
Space group	$P6_522$	$P2_12_12_1$
Unit cell (Å)		
a, b, c (Å)	73.16, 73.16, 226.27	45.33, 96.33, 189.36
α, β, γ (°)	90, 90, 120	90, 90, 90
Resolution (Å)	2.20	2.54
Anisotropic resolution (Å)	–	2.54 II a, b 2.96 II c
Rsym	0.08 (1.00)	0.14 (0.75)
$\langle I \rangle / \langle \sigma I \rangle$	24.3 (2.0)	16.2 (2.0)
Unique reflections	22,370 (2,178)	28,012 (1,279)
Completeness (%)	98.9 (100.0)	99.4 (93.2)
Redundancy	11.2 (10.2)	10.0 (7.4)
Wilson B-factor ($Å^2$)	67.0	48.6
Refinement		
Resolution (Å)	28.6 – 2.2	48.2 – 2.9
No. reflections (test set)	22,262 (1,114)	19,160 (959)
R_{work} / R_{free} (%)	22.3 / 28.1	27.2 / 31.7
Number of non-H atoms	2,578	5,266
Protein	2,498	5,086
Ligand/ion	33	66
Water	47	114
Average B-factor ($Å^2$)	84.6	54.9
rms deviations		
Bond lengths (Å)	0.016	0.003
Bond angles (°)	1.601	0.584
Ramachandran *favored/allowed/disallowed* (%)	95.4 / 4.6 / 0.0	95.0 / 5.0 / 0.0
Molprobity score	1.96 (87^{th} percentile)	1.66 (100^{th} percentile)
Molprobity clashscore	7.51 (96^{th} percentile)	2.99 (100^{th} percentile)

*Values in parentheses are for highest-resolution shell